The influence of phase angle, strain range and peak cycle temperature on the TMF crack initiation behaviour and damage mechanisms of the nickel-based superalloy, RR1000

Jonathan Jones, Mark Whittaker, Robert Lancaster, Stephen Williams

PII: S0142-1123(17)30045-2
DOI: http://dx.doi.org/10.1016/j.ijfatigue.2017.01.036
Reference: JIJF 4226

To appear in: *International Journal of Fatigue*

Received Date: 31 October 2016
Revised Date: 23 January 2017
Accepted Date: 25 January 2017

Please cite this article as: Jones, J., Whittaker, M., Lancaster, R., Williams, S., The influence of phase angle, strain range and peak cycle temperature on the TMF crack initiation behaviour and damage mechanisms of the nickel-based superalloy, RR1000, *International Journal of Fatigue* (2017), doi: http://dx.doi.org/10.1016/j.ijfatigue.2017.01.036

The influence of phase angle, strain range and peak cycle temperature on the TMF crack initiation behaviour and damage mechanisms of the nickel-based superalloy, RR1000

Authors:

Jonathan Jones, Institute of Structural Materials; Swansea University; Singleton Park; Swansea, UK, SA2 8PP – jonathan.p.jones@swansea.ac.uk

Mark Whittaker, Institute of Structural Materials; Swansea University; Singleton Park; Swansea, UK, SA2 8PP – m.t.whittaker@swansea.ac.uk

Robert Lancaster, Institute of Structural Materials; Swansea University; Singleton Park; Swansea, UK, SA2 8PP – r.j.lancaster@swansea.ac.uk

Stephen Williams, Rolls-Royce plc; Elton Road; Derby DE24 8BJ, UK – steve.williams@rolls-royce.com

Abstract

Thermo-mechanical fatigue (TMF) tests including 0°, 90°, -90°, 45° -135° and -180°, phasing (φ) between mechanical loading and temperature were undertaken on a polycrystalline nickel-based superalloy, RR1000. Mechanical loading was employed through strain control whilst 300-700 °C and 300-750°C thermal cycles were achieved with induction heating and forced air cooling. Mechanical strain ranges from 0.7 to 1.4% were employed. Results show that, for the strain ranges tested, TMF life is significantly affected by the employed phase angle. Furthermore the strain range and peak cycle temperature used has a substantial influence on the significance of dominant damage mechanisms, and resultant life. Various metallographic examination techniques have outlined that the dominant damage mechanisms are creep deformation at higher temperatures and early cracking of oxide layers at lower temperatures.

Introduction

It has long been known that TMF loading can be more damaging than typical isothermal fatigue (IF). Increasing operating temperatures to improve cycle efficiency and mechanical loading to enhance performance in conjunction with weight reduction strategies that include

thinner disc rims have led not only to more aggressive thermal gradients, and hence TMF cycles, but also to the requirement for assessment of the behaviour of components for which TMF was not previously considered significant.

The publication of the ASTM E2368-10[1] and more recently ISO12111:2012[2] strain controlled thermo-mechanical fatigue standards, emphasises the significance of dynamic temperature effects on material fatigue behaviour. However, uncertainty still remains with regards to how accurately temperature can be measured and controlled during these tests. Accurate temperature and loading control is imperative, as it enables the desired phasing or shift between the temperature and mechanical strain, known as the phase angle (ϕ).[3] The author has undertaken further work to enhance the accuracy and repeatability of temperature control during such dynamic tests as TMF.[4]

Under elevated temperature conditions, the total TMF damage is composed of fatigue, creep and environmental elements. Depending on the phase angle, the relative contributions of these may vary.[5] A consequence of the additional variable, ϕ, is the enormous number of potential TMF conditions, however a limited number are outlined to be of use.[3] Typical studies consider TMF in one of two ways; an In-Phase (IP) ($\phi = 0°$), or Out-of-Phase (OP) ($\phi = -180°$) condition, where the maximum and minimum loading on the material coincides with the maximum and minimum temperature respectively.

Despite the vast number of test conditions that can be employed, limited literature considers the phase angles that exist between the generic IP and OP extremes, representing the in service loading conditions more accurately in some cases. Typical alternative phase angles are, Clockwise Diamond (CD, $\phi=90°$), Counter Clockwise Diamond (CCD, $\phi= -90°$), Clockwise (CW, $\phi=45°$) and Counter Clockwise (CCW, $\phi = -135°$). The phase angle

(ϕ = -135°) is the closest representation of the stress condition seen in turbine blades and disc components through high temperature transients.[6]

Resultant TMF failure crack growth mechanisms in nickel alloys have been reported as being predominantly pure intergranular fracture under IP loading, whilst under OP and alternate loading cycles, (e.g. Clockwise Diamond, ϕ = 90°) failure is primarily transgranular mixed mode.[5, 7] Under IP loading a polycrystalline structure produces inter crystalline cracks, whilst OP conditions cracks grow only along the crystallographic {111} planes.[8] Transitions between intergranular and transgranular cracking damage mechanisms have been reported with the increase in temperature.[9] This has been attributed to the increased oxidation damage at the grain boundaries ahead of the crack tip as the temperature is increased.[10]

The combination of both high and low temperature dislocation movements and therefore crack growth mechanisms associated with isothermal fatigue exist in TMF cycles.[11] Enhanced oxidation growth can result from the diverse damage mechanisms interacting and working in parallel. Oxidation can not only limit life on its own, but also interacts with creep and fatigue mechanisms that need to be considered.[11,12] Brittle surface oxide crack initiation under TMF loading has been reported in literature.[11,12] A further influence of TMF is the possibility of microstructural change leading to local strength reductions.[8, 12] The structure of γ'-phase at the surface can be denuded, resulting from the reduction of oxide forming elements. After prolonged periods of high temperature exposure this can result in a reduced resistance to crack propagation.[12]

This study considers the life, cyclic deformation and damage behaviour under diverse TMF loading conditions. The objective is to obtain a better understanding about how particular damage mechanisms vary and interact with phase angle, peak cycle temperature and strain range and what influence this has on the resultant life of the components.

Experimental Testing

The γ' strengthened polycrystalline Ni-based superalloy, RR1000, was considered in this investigation. The alloy is produced through a powder metallurgy route and strengthened through the precipitation of a secondary γ' phase (Ni_3 (Al, Ti, Ta)) from an FCC γ matrix. The desired average γ grain size of 4-8μm was achieved through a sub-solvus solution heat treatment, leaving irregular shaped primary γ' particles (1-5μm in size) on grain boundaries.

Tubular hollow test specimens were utilised for testing, Fig.1a. Tubular specimens had a 35mm gauge length with internal and external diameters of 8mm and 10mm respectively. The temperature distribution across the test specimen was shown to conform within the guidelines defined in the ISO and ASTM strain control TMF standards and previous work.[1, 2] Standard pre-requisite tests including modulus checks, thermal compensation definitions and zero stress trials were also performed to ensure test viability.

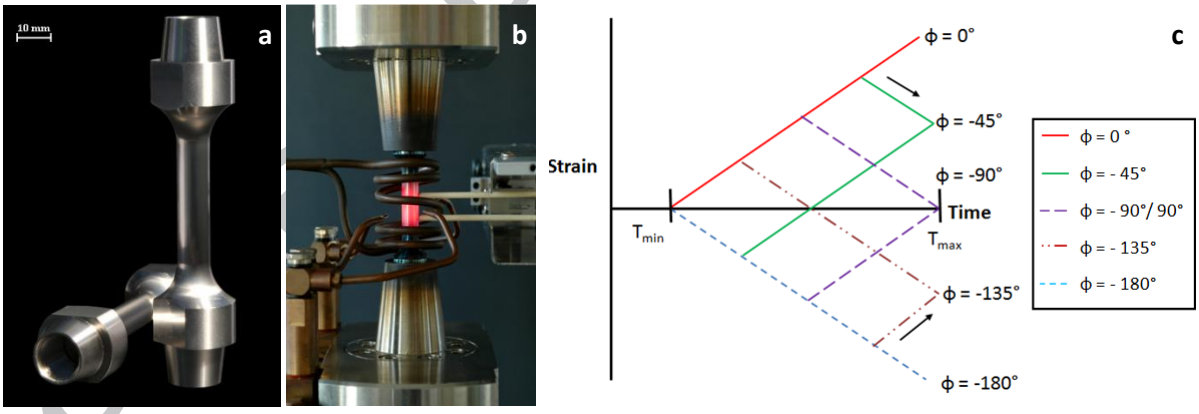

Figure 1. a) Hollow TMF test specimen. b) Strain control TMF test facility. c) Phase angles (ϕ) and directions employed.

All TMF tests were undertaken on an ESH 100kN tension-torsion servo-hydraulic test machine under strain-controlled conditions. The system utilised radio-frequency (RF) induction heating through a water cooled copper coil to achieve rapid heating rates. Equivalent rapid cooling rates are achieved by use of forced air cooling both through the

centre of the hollow specimen and externally upon its surface though air jets, Fig1.b. The temperature was measured by an IMPAC IP10 optical pyrometer which was connected to a two way control system. Extension was controlled and measured using a 12mm gauge MTS high temperature extensometer with the total strain and thermal cycles synchronised and controlled by a closed loop computer to facilitate the phasing between mechanical and thermal loading.

Due to the difficulty of performing direct temperature measurement from the internal surface in situ, only anecdotal evidence for the lack of temperature gradients can be provided. However, the authors feel that these checks are quite robust. Benchtop temperature calibrations were undertaken using induction heating upon a sectioned specimen, internal and external TC's were within ±2°C when compared against each other at the peak cycle temperature. Previously in alternative experiments using 7x7mm solid specimens, internal temperatures were measured through a thermocouple inserted into a drilled hole in the centre of the specimen; once more temperature differences between the internal and external surfaces were minimal, being within ±2°C. It is therefore felt that the combination of the thin walled tubular specimens, coupled with the high thermal conductivity of the alloy, reduce the susceptibility of the specimens to significant thermal gradients. Furthermore, no direct influence on the specimen failures has been detected, with no preference seen for failure from the internal or external surface.

In order to evaluate the effect of phase angle on the TMF life of RR1000, tests were performed using ϕ =0°(IP), 45°(CW), 90°(CD), -90°(CCD), -135°(CCW), and -180^0(OP) phasing between mechanical strain and temperature, Fig.1c. Mechanical strain ranges from $\Delta\varepsilon$= 0.7 to 1.4% were employed, resulting in strain R ratios varying between 0 and -∞ depending on the phase angle ϕ. Triangular thermal cycles employed were 300 - 700°C and

300 - 750°C, over a thirty second interval with equal, fifteen second heating and cooling stages, equating to ~26°C/s^{-1} and 30°C/s^{-1} respectively. These test conditions have been chosen as they are directly relevant to the industrial sponsor, Rolls-Royce plc, commercial applications. Failure was defined as the number of cycles to achieve a 10% drop in stress from the stabilised peak stress value, at which point a detectable engineering sized crack is assumed to be present in the sample.

Results

Figure 2 presents the isothermal and TMF data, normalised by a mid-range ($\Delta\varepsilon$=1.1%) isothermal test at 700°C to illustrate the detrimental effect of TMF compared to isothermal behaviour. The greatest life is achieved by the isothermal LCF tests at the minimum TMF cycle temperature (300°C). Isothermal LCF tests undertaken at the peak TMF cycle temperatures (700°C and 750°C) yielded a greater life when compared to the IP TMF tests. Life increases in the sequence IP < OP under the 300-700°C temperature range, at strain ranges $\Delta\varepsilon > 0.8\%$. However, at lower strain ranges, $\Delta\varepsilon \leq 0.8\%$, the life of IP TMF approaches and finally exceeds that of the OP TMF. A crossover of the IP and OP curves appears at approximately $\Delta\varepsilon = 0.8\ \%$, where life now increases in the sequence OP < IP, Fig.2a

Increasing the maximum cycle temperature by 50°C to 750°C has a significant effect on OP lives, reducing them by an order of magnitude. IP lives, although reduced by the increase in peak cycle temperature, are not significantly affected. Under this 300-750°C thermal cycle, OP life is significantly less than IP at strain ranges $\Delta\varepsilon < 1.0\ \%$, where again a crossover of the IP and OP curves appears.

The lifetimes of the additional phase angles sit between those of the IP and OP extremes, being the most and least damaging respectively at strain ranges $\Delta\varepsilon > 0.8\%$, Fig.2b. Lifetimes of $\phi = -135°$ tests are generally the lowest of the additional phase angles. Results of diamond

tests fall into a very similar scatter band, having similar lifetimes across all conditions. At strain ranges above $\Delta\varepsilon > 0.8$ %, Diamond 90°/-90° lifetimes are greater than that of the CW45° and CCW-135° tests, again there is a crossover in TMF life curves . At strain ranges $\Delta\varepsilon \leq 0.8$ %, the CW45° condition holds a similar curve to that of IP condition under the same thermal cycle; the CW45° cycle has a far superior life, below strain ranges of $\Delta\varepsilon \leq 0.8\%$.

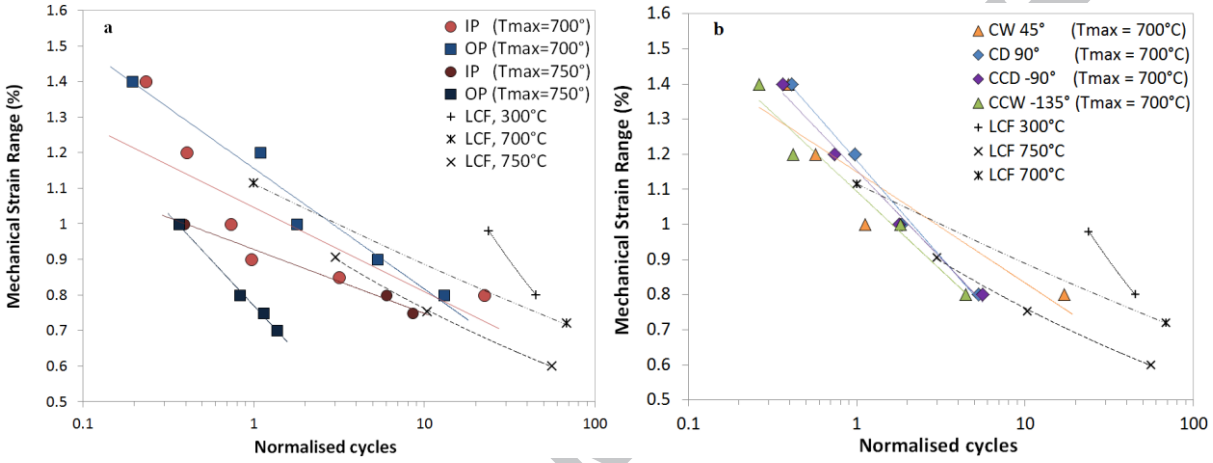

Figure 2. a) Curves of mechanical strain vs. cycles to failure for IP and OP TMF conditions b) CW45°, CD, CCD and CCW-135° TMF condition. Tests used 300-700°C and 300-750°C thermal cycles. Isothermal LCF curves are also shown for the TMF thermal cycle extremes, 300, 700 and 750°C.

First, last and half-life ($N_f/2$), stress-mechanical strain TMF hysteresis loops are given in Fig.3 for a) IP and b) OP conditions at $\Delta\varepsilon = 0.8\%$, under both the 300-700°C and 300-750°C thermal cycles. During the initial cycle, monotonic plastic deformation takes place at peak cycle temperature under tensile stresses during IP conditions (R, = 0), and under compressive stresses during OP conditions (R, = -∞). Under both IP and OP cycling, as expected TMF life increases with decreasing strain range and hence the resultant peak cycle stress. However it is obvious that the cyclic stress response to TMF depends not only on the strain range but also on the phase shift between temperature and strain.

The stress response to phase shift is ever more pronounced with the increase in peak cycle temperature by 50°C as shown for OP cycles in Fig.3c. Stress relaxation of the maximum compressive stress at high temperature and thus resultant maximum tensile stress evolution under OP, is far more pronounced than the tensile stress relaxation under IP. Maximum tensile stresses at the end of the first cycles were 400 and 700MPa using peak cycle temperatures of 700 and 750°C respectively. However, only a 100MPa relaxation of the minimum compressive stress was found between the first loops of the IP 700 and 750°C peak cycle temperature tests.

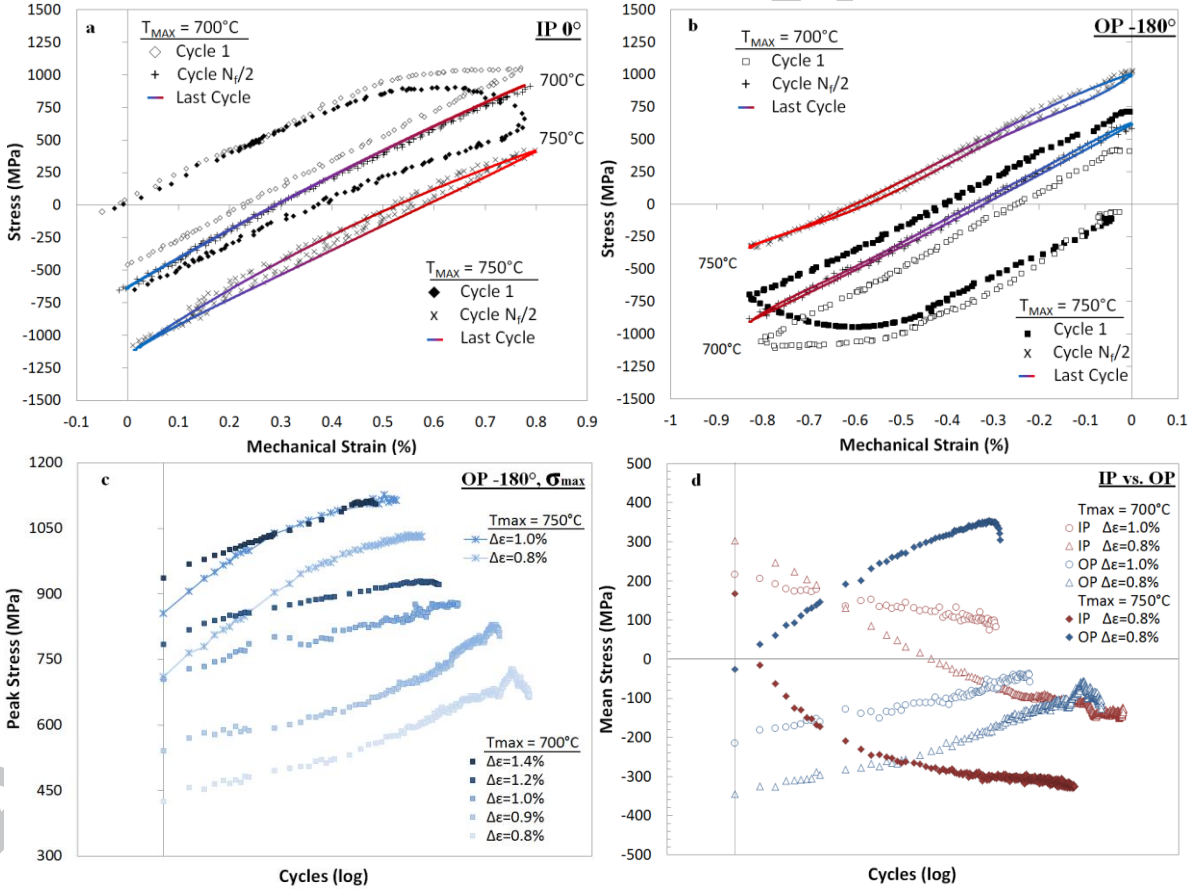

Figure 3. Results from 300-700°C and 300-750°C thermal cycles, first, stabilised and last TMF hysteresis loops at Δε=0.8% under, a) IP and b) OP loading. **c)** Cyclic peak stress response curves of OP TMF tests. d). Cyclic mean stress evolution of IP and OP TMF tests at ε=0.8% and 1.0%.

Differences in the rate at which hardening and softening occurs under OP and IP loading respectively is visible across all strain ranges tested. Rapid relaxation occurs during the initial cycles under IP loading and the rate of this relaxation is then progressively reduced with continued cycling, approaching stress saturation towards the end of the test. No such reduction in hardening rate is observed in OP tests, where continued hardening persists through to failure. A result of this inelastic deformation is that during the subsequent cycles the stress evolves further to a tensile mean stress under OP loading and compressive mean stress during IP loading, Fig.3d.

Under Diamond 90°/-90°conditions, the stress-temperature hysteresis loops resemble a diamond shape, Fig.4a. For both, Diamond 90° and -90°, the highest stress appears around the mean temperature (500°C), whereas at the highest and lowest temperatures the stress magnitude is small. In Diamond 90° tests, tensile loading takes place in the low temperature regime while compressive loading occurs in the high temperature regime. In Diamond -90° tests it is the opposite situation.

Under CW45° and CCW-135° conditions, the highest stress appears at moderately high temperatures (600°C) and moderately low temperatures (400°C) respectively, whereas at the lowest stress these temperatures are reversed. In CW45° tests, tensile loading takes place in the high temperature regime, while compressive loading occurs in the low temperature regime, similar to IP loading. In CCW-135° tests it is the opposite situation and is closer to OP loading conditions. Stress relaxation during CW45° cycling leads to a slight shift of the hysteresis loops towards the compressive region, as a result of the induced maximum tensile stress during the high temperature half cycle being moderately reduced, signifying cyclic softening, Fig.4c. Cycling generally exhibits initial softening that is followed by saturation at an increasing degree as the strain range is reduced.

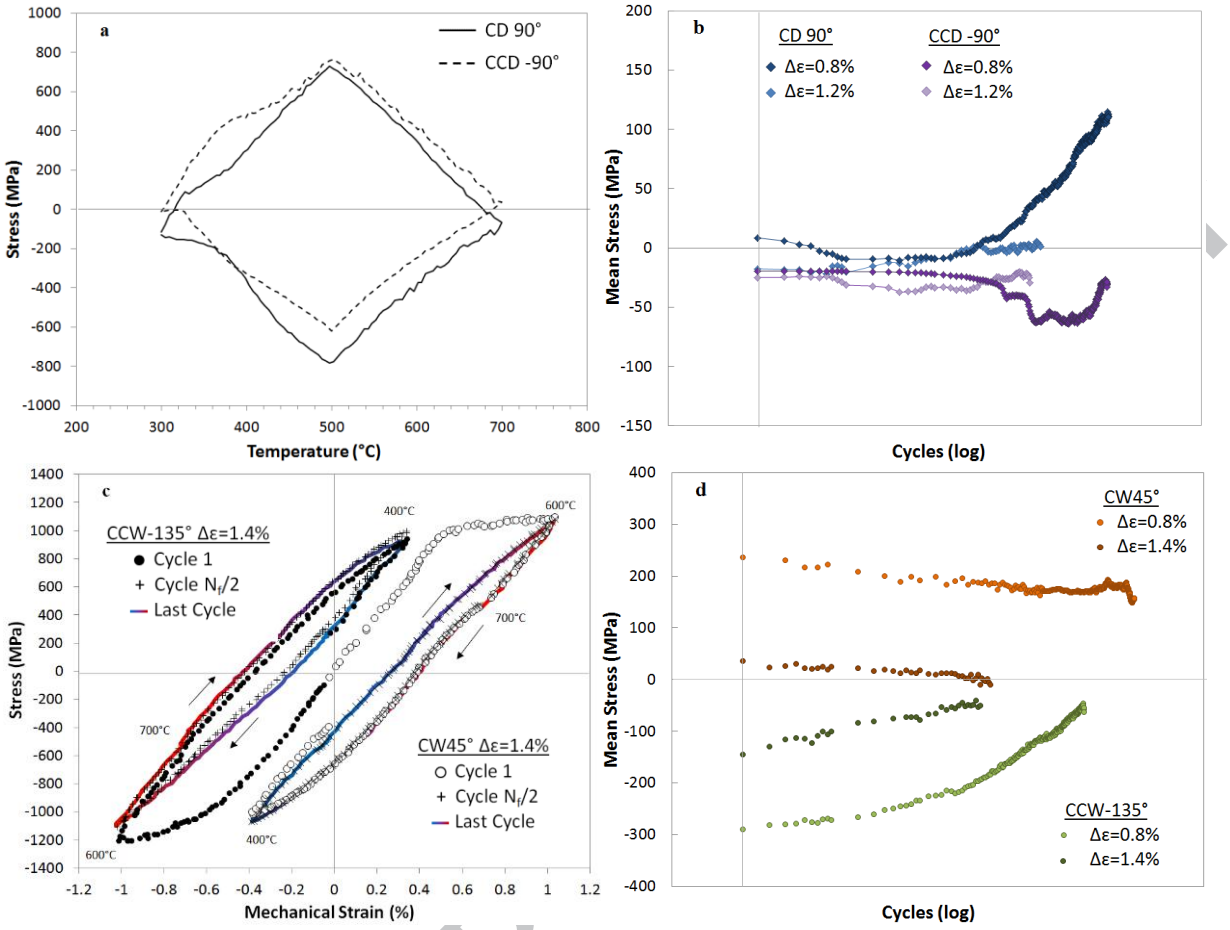

Figure 4. Results from 300-700°C thermal cycle tests, a) Influence of cycle direction on the stabilised TMF stress-temperature hysteresis loops at Δε=0.8%, under Diamond 90°/-90° loading. b) Cyclic mean stress evolution of Diamond 90°/-90° TMF tests at Δε=0.8% and 1.0%. c) CW45° and CCW-135° first, stabilised ($N_f/2$) and last TMF hysteresis loops at Δε=0.8%. d). CW45°/CCW-135° TMF test cyclic mean stress evolution at Δε=0.8% and 1.0%.

Inelastic deformation during CCW-135° cycling shifts hysteresis loops into the tensile region. Initial hardening continues to progress with higher numbers of cycles with no subsequent saturation reached before failure, with evidence of cyclic hardening. The evolution of cyclic mean stress under these loading conditions is shown in Fig.4d.

Evidence of predominantly pure intergranular cracking is found under IP conditions, Fig.5a), whilst a mix of intergranular and transgranular is present for OP, Diamond 90°/-90°, CW45°

and CCW-135°, Fig.5b). Damage is predominantly intergranular under CW45° moving progressively to more predominantly transgranular under OP in the order CW45°, CCD-90°, CD90°, CCW-135°, OP. Cracks under OP appear straight and sharp, Fig5c/e), cracks in Diamond 90°/-90° tested specimens exhibit a wavy morphology. Intergranular cracks are found from IP, and CW45° loading in the bulk that have no connection to the surface, whilst a connection was generally found under OP, Diamond 90°/-90° and CCW-135° loading.

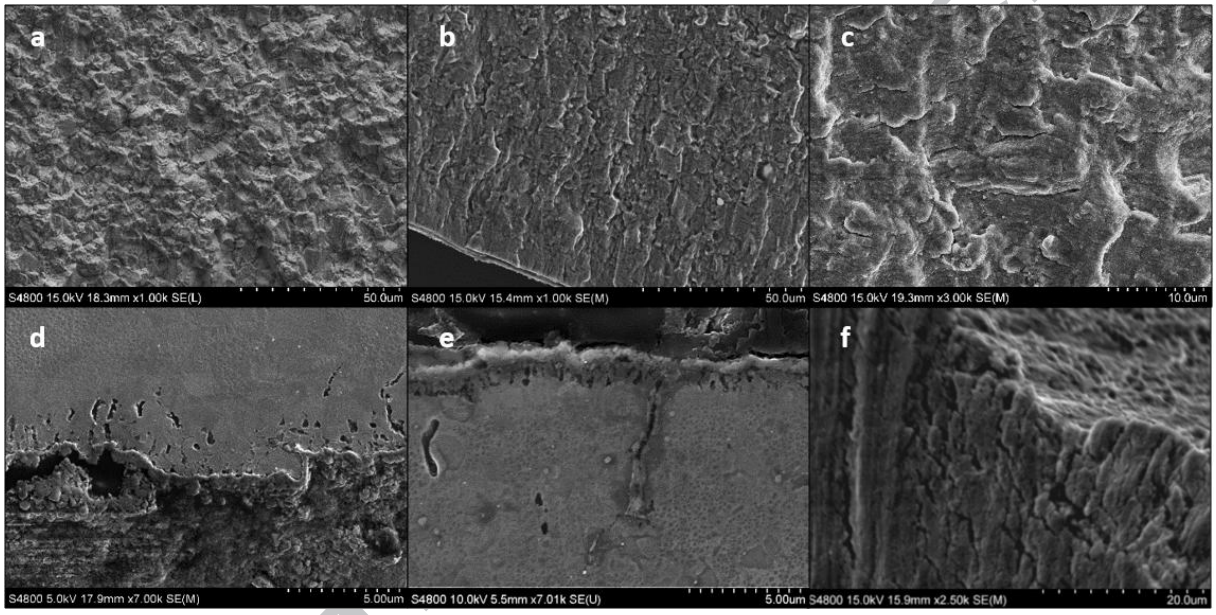

Figure 5. Fractured TMF specimen SEM surface images of a) IP, and b), c) OP tests showing intergranular, with evidence of sub surface cracking and predominantly transgranular with striations visible, damage mechanism respectively. IP Intergranular surface oxide damage is shown in d) with transgranular and surface oxide cracking under OP loading shown in e) and f).

Discussion

Comparing TMF lives with those of equivalent isothermal temperature LCF tests, by and large TMF test conditions across all strain ranges and peak cycle temperatures proved more detrimental to cycle life, especially at low mechanical strain ranges, Fig.2a,b. Dynamic cycle temperatures associated with TMF have been previously attributed to this reduction in life.[8 13] Moreover local thermal stress mismatches between phases in the alloy can cause local thermal

fatigue damage during the prolonged TMF cycles.[14] Crack initiation and propagation in TMF has also typically been shown to be promoted by creep and enhanced oxidation behaviour.

The TMF life is governed by the active dominant damage mechanism. Under the 700°C peak cycle temperature at strain ranges greater than 0.8%, IP lives are less than OP lives Fig.2a, maintaining the assumption that the longer the duration of cyclic life spent under high temperature tensile conditions, the lower the resulting specimen life with creep and fatigue the more dominant damage mechanisms. In IP tests, creep and oxidation damage on grain boundaries lead to accelerated intergranular crack propagation, Fig.5a,d. This is considered to result from the fact that the creation of voids and the growth of cracks generally occur under tensile conditions and this effect is found to increase as the temperature increases.

The observed cyclic shift of the stress level in IP and OP tests, Fig.3a,b, is a consequence of gradual inelastic strain accumulation due to creep deformation and resultant stress relaxation in the high temperature regime where the elastic modulus is lower. In IP tests, this leads to a gradual shift of the hysteresis loop towards the compressive region. As a result the induced maximum tensile stress during the high temperature half cycle is reduced, signifying cyclic softening. Generally, a high rate of softening is exhibited during the early stages of the test. The rate of softening is then reduced with continued cycles, this effect is enhanced with decreasing stain range.

Inelastic deformation during OP cycling shifts hysteresis loops into the tensile region. Relaxation of compressive stress occurs at the peak cycle temperature, resulting in the evolution of a maximum tensile stress by the end of the first low temperature half cycle. Slow initial cyclic hardening then continues to progress with higher numbers of cycles with no subsequent saturation reached before failure, Fig.3c. As a result, compressive and tensile mean stresses are obtained for IP and OP tests respectively, Fig.3d.

The stress shift during TMF is significantly influenced by the phase angle employed and enhanced with an increase in peak cycle temperature, Fig 6a. The stress shifts continue up to the point when either the stress induced at high temperatures has become too low to drive further creep or when the cyclic yield stress at T_{min} is reached and the plastic strain due to stress relaxation is offset by low temperature plasticity and dislocation glide. At higher strain ranges, the yield stress at T_{min} is reached earlier, thus, the shift is less pronounced or does not occur at all. Hence, an increase of strain range in IP tests results in a relatively high increase of tensile stress and therefore in a high increase of the dominant creep damage. In OP tests however, the saturated maximum stress has a lower sensitivity to strain range since an increase of strain range gives only a moderate increase of maximum stress and damage to the oxide layers. This is the reason why in Fig.2a, the slope of the IP TMF curve is considerably shallower than the slope of the OP TMF curve.

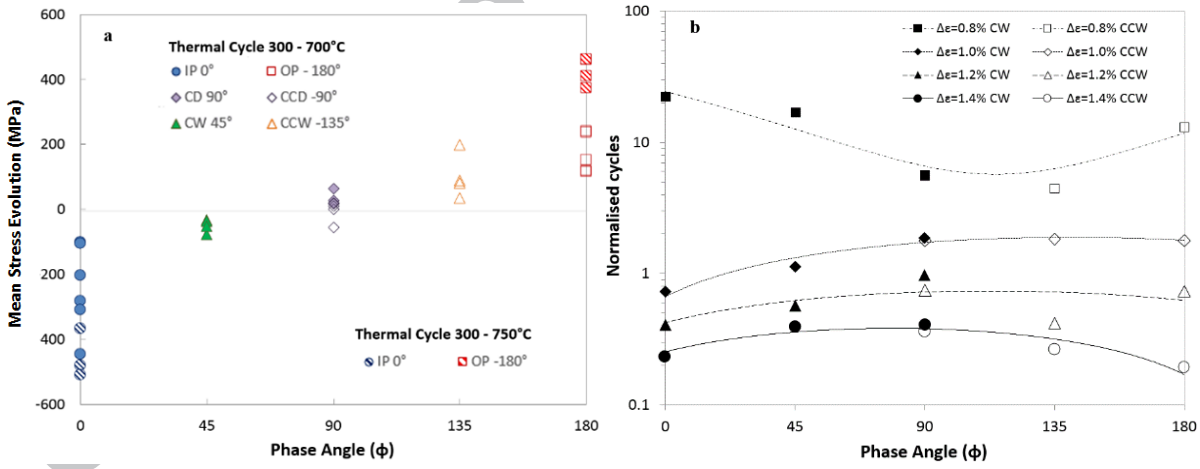

Figure 6.a) Relationship between mean stress evolution (difference between cyclic mean stress of 1st and stabilised cycles) and phase angle in the temperature range 300-700°C. b) Relationship between TMF life and phase angle over various stain ranges under the 300-700°C thermal cycle.

In OP tests, high tensile stresses appear at low temperatures when the surface oxide layer has the lowest ductility. This may lead to early crack initiation on the surface oxide layer and increased transgranular crack propagation due to the high stress at low temperature and

therefore reduce the life.[13,15] The transgranular fracture surface morphologies, Fig.5b/c, and high amount of surface oxide cracks found on OP specimen surfaces, Fig.5e, support this assumption. Furthermore, the high tensile stress in OP tests leads favours the propagation of one dominant crack.[16] This is why most of the cracks in OP tests remain relatively short. As the crack surface is closed and isn't actively growing under compressive loading at maximum temperature, fatigue striations formed are less oxidised and are clearly visible.

In IP tests, tensile stress at high temperatures promotes creep damage in form of cavities and wedge type cracks on grain boundaries, promoting intergranular cracking, Fig.5a/d. During the compressive half cycle the temperature is too low to sinter out the cavities. This gives rise to continuously increasing grain boundary damage during tensile half cycles eventually leading to cracks that appear often in the bulk material whereas relatively few surface cracks initiate. Internal intergranular cracks after IP-TMF loading have been reported for similar materials.[10] Furthermore, the grain boundaries may be weakened by preferential oxidation as the crack is open at high temperature under tension[16]. Crack propagation along the damaged grain boundaries is facilitated and the crack growth rate is increased.

A crossover in mechanical strain range-life curves under the 300-700°C thermal cycle of IP and OP conditions occurs at low strain ranges, approximately $\Delta\varepsilon = 0.8\%$, Fig.2a. The location of this crossover has been found to vary depending on the material, strain range and cycle temperature, all of which interact to influence and promote the dominant damage mechanism.[8,12,17,18] The effect of phase angle on life is given in Fig.6b, where the crossover between IP and OP performance is clearly visible around $\Delta\varepsilon = 0.8\%$.

The crossover may be explained by the varying levels of creep and oxidation. The fatigue life of the alloy is reduced at high mechanical strain ranges and therefore less time is spent at elevated temperature. As a result a less than significant amount of oxidation is accrued.

Additionally, under IP conditions, creep damage is significant, resulting in the reduced life of IP conditions over OP at high mechanical strain ranges. Inelastic strain under low mechanical strain ranges is significantly less, so most damage resulting from creep can be neglected.[17] Therefore the potential for oxidation dominated rupture under low temperature tension in combination with the enhanced evolution of tensile mean stress promoting crack initiation and propagation can be accountable for the reduction in OP life over IP in lower mechanical strain ranges.[7,8]

The varying openings of the stress-temperature hysteresis loops in the tensile and compressive half cycle of Diamond 90°/-90° tests can be attributed to the temperature dependence of the elastic modulus, Fig.4a. In Diamond 90°/-90° tests, both minimum and maximum stress appear in the region of the mean temperature, so there is no asymmetry of the deformation mechanisms and no significant stress level shift and resultant evolution of mean stress occurs, Fig 4b. Lives of Diamond 90°/-90° tests are greater than IP and less than OP tests above strain ranges of $\Delta\varepsilon$=0.8%. Since the max and min strain appears at the mean temperature of 500°C, it may be assumed that the resulting life is comparable with isothermal fatigue life at T = 500°C. Under these conditions the tensile stress at high temperatures seems too low to induce creep damage. Thus, the grain boundaries potentially do not suffer critical creep damage, hence cracks propagate in mainly a transgranular mannor.

Accelerated crack initiation on the oxide layer presumably also occurs in CD90° tests when tensile loading takes place in a lower temperature region than CCD-90°. However no evidence was found to suggest that this is a critical damge mechansim under these condtions as similar lifes were achieved, suggesting that cycle direction in the diamond cycles had no significant effect on life, Fig 2b, findings consistent with previous work.[18] A wavy morphology of the longer cracks in both Diamond 90°/-90° tests suggest that they propagated

by repeated plastic blunting and re-sharpening, consistent with previous work.[15] Accordingly, the damage in Diamond 90°/-90° tests is governed by cyclic plasticity occurring predominantly in the mean temperature regime.

CW45° and CCW-135° cycles follow similar trends with decreasing strain range as the IP and OP extremes respectively, Fig.2b, as does the cyclic stress response, with cyclic softening and hardening evident under CW45° and CCW-135° respectively, Fig.4c and d.

Conclusions

In general the TMF conditions tested are more detrimental upon life than the equivalent IF conditions. The phase angle employed has been found to have significant influence on the cycle mean stress evolution, deformation, and damage behaviour, significantly influencing TMF life. Moreover the strain range and/or peak cycle temperature affects the degree of this influence.

Stress relaxation in the high temperature cycle regions results in cyclic softening under IP loading and cyclic hardening under OP loading. At higher mechanical strain ranges above $\Delta\varepsilon > 0.8\%$, IP conditions are the most detrimental on TMF life with OP the least. Lifetimes of the alternate phase angle conditions tested sit between the higher and lower lives of the OP and IP extremes respectively, in the general sequence CCW-135° < CW45° < CD90°≈CCD-90°.

At lower mechanical strain ranges below $\Delta\varepsilon \leq 0.8\%$, OP conditions are now more detrimental than IP, with a crossover between mechanical strain - life curves and thus the more dominant damage mechanism occurring at approximately $\Delta\varepsilon = 0.8\%$.

At $\Delta\varepsilon>0.8\%$, the dominant damage mechanism has been identified as creep damage on grain boundaries, generating accelerated intergranular cracking that is enhanced by the coinciding high temperature and tensile stress under IP loading. At $\Delta\varepsilon<0.8\%$, accelerated surface oxide

crack initiation at low temperature is the dominant mechanism under OP loading, accelerated by the evolving tensile mean stress.

A similar response is seen in CW45° and CCW-135° tests with the former closer to IP and the latter closer to OP conditions. In Diamond 90°/-90° tests neither of these damage mechanisms is pronounced, and with no asymmetry of the deformation mechanism, no significant mean stress is accumulated and as a result lifetimes are extremely similar with no effect of cycle direction shown.

Increasing the peak cycle temperature by 50°C enhances the evolution of cyclic mean stress, reducing OP lifetimes significantly whilst IP lifetimes, although reduced, remain relatively unaffected. Again a crossover of IP and OP life curves and more dominant damage mechanism occurs, now at an increased strain range of approximately $\Delta\varepsilon = 1.0\%$.

Acknowledgements

The current research was funded under the EPSRC Rolls-Royce Strategic Partnership in Structural Metallic Systems for Gas Turbines (grants EP/H500383/1 and EP/H022309/1). The provision of materials and supporting information from Rolls-Royce plc is gratefully acknowledged.

References

1. Standard Practice for Strain Controlled Thermomechanical Fatigue Testing, E2368-10, ASTM, 2010.
2. Metallic materials, Fatigue testing, Strain-controlled thermomechanical fatigue testing method, 12111, ISO, 2011.
3. P. Hahner, C. Rinaldi, V. Bicego, E. Affeldt, T. Brendel, H. Andersson, T. Beck, H. Klingelhoffer, H. Kuhn, and A. Koster, Research and development into a European code of practice for strain controlled thermo-mechanical fatigue testing, *Int. J. Fatigue*, 2008, **30**(2), 372-381.
4. J. P. Jones, S. P. Brookes, M. T. Whittaker, R. J. Lancaster, and B. Ward: 'Assessment of Infrared Thermography for Cyclic High-Temperature Measurement and Control', 4th

Evaluation of Existing and New Sensor Technologies for Fatigue, Fracture and Mechanical Testing, Toronto, 2015, ASTM International, 186-206.
5. S. Pahlavanyali, G. Drew, A. Rayment, and C. Rae, Thermo-mechanical fatigue of a polycrystalline superalloy: The effect of phase angle on TMF life and failure, *Int. J. Fatigue*, 2008, **30**(2), 330-338.
6. J. H. E.E. Affeldt, U. Huber and H. Lundblad, Analysis of Thermal Gradients during Cyclic Thermal Loading under High Heating Rates, *Thermomechanical Fatigue Behaviour of Materials*, 2003, **4**.
7. G. P. T. Beck, K.-H. Lang, D. Lohe, Thermal-mechanical and isothermal fatigue of IN 792 CC, *Materials science & engineering A*, 1997, **A234-236**, 719-722.
8. D. A. Boismier and H. Sehitoglu, Thermo-Mechanical Fatigue of Mar-M247: Part 1—Experiments, *J. Eng. Mater. Technol.*, 1990, **112**(1), 68-79.
9. F. Daus, H. Y. Li, G. Baxter, S. Bray, and P. Bowen, Mechanical and microstructural assessments of RR1000 to IN718 inertia welds – effects of welding parameters, *Mater. Sci. Technol.*, 2007, **23**(12), 1424-1432.
10. Y. Kadioglu and H. Sehitoglu, Thermomechanical and isothermal fatigue behavior of bare and coated superalloys, *Engineering Materials and Technology*, 1996, **118(1)**, 94-102.
11. C. Sommer, M. Bayerlein, and W. Hartnagel: 'Deformation and failure mechanisms of DSCM247LC under TMF and LCF loading', 81st AGARD Conference on Thermal Mechanical Fatigue of Aircraft Engine Materials, Canada, 1995, 11-12.
12. M. Arana, J. M. Martínez-Esnaola, and J. Bressers: 'Crack Propagation and Life Prediction in a Nickel-Based Superalloy under TMF Conditions', in 'Fatigue under Thermal and Mechanical Loading: Mechanisms, Mechanics and Modelling', (eds. J. Bressers, et al.), 393-402; 1996, Springer Netherlands.
13. H. Sehitoglu and D. A. Boismier, Thermo-Mechanical Fatigue of Mar-M247: Part 2—Life Prediction, *J. Eng. Mater. Technol.*, 1990, **112**(1), 80-89.
14. L. H. Qian, Z. G. Wang, H. Toda, and T. Kobayashi, Effect of reinforcement volume fraction on the thermo-mechanical fatigue behavior of SiCW/6061Al composites, *Materials Science and Engineering: A*, 2003, **357**(1–2), 240-247.
15. H. U. Hong, J. G. Kang, B. G. Choi, I. S. Kim, Y. S. Yoo, and C. Y. Jo, A comparative study on thermomechanical and low cycle fatigue failures of a single crystal nickel-based superalloy, *Int. J. Fatigue*, 2011, **33**(12), 1592-1599.
16. Z. W. Huang, Z. G. Wang, S. J. Zhu, F. H. Yuan, and F. G. Wang, Thermomechanical fatigue behavior and life prediction of a cast nickel-based superalloy, *Materials Science and Engineering: A*, 2006, **432**(1-2), 308-316.
17. L. Z. He, Q. Zheng, X. F. Sun, H. R. Guan, Z. Q. Hu, A. K. Tieu, C. Lu, and H. T. Zhu, High temperature low cycle fatigue behavior of Ni-base superalloy M963, *Materials Science and Engineering: A*, 2005, **402**(1–2), 33-41.
18. S. Guth, S. Doll, and K.-H. Lang, Influence of phase angle on lifetime, cyclic deformation and damage behavior of Mar-M247 LC under thermo-mechanical fatigue, *Materials Science and Engineering: A*, 2015, **642**, 42-48.

Highlights - The influence of phase angle, strain range and peak cycle temperature on the TMF crack initiation behaviour and damage mechanisms of the nickel-based superalloy, RR1000

1. Thermo-mechanical fatigue testing of a nickel superalloy across multiple strain ranges
2. Six diverse phase angles between 0° to -180° and various peak cycle temperatures are used.
3. Evolution of mean stresses and the influence of oxidation upon failure mechanisms are assessed.
4. Relationships between test life, phase angle and mean stresses are realised.